Available online at www.sciencedirect.com
SCIENCE DIRECT®
PHYTOCHEMISTRY
Phytochemistry 66 (2005) 2800–2814
www.elsevier.com/locate/phytochem

Molecules of Interest

Sugar beet (*Beta vulgaris*) pectins are covalently cross-linked through diferulic bridges in the cell wall

Marie-Christine Ralet *, Gwénaëlle André-Leroux [1], Bernard Quéméner, Jean-François Thibault

Unité Biopolymères Interactions Assemblages, Institut National de la Recherche Agronomique, rue de la tsaven Géraudière B.P. 71627, 44316 Nantes Cedex 03, France

Received 19 July 2005; received in revised form 28 September 2005
Available online 17 November 2005

Abstract

Arabinan and galactan side chains of sugar beet pectins are esterified by ferulic acid residues that can undergo in vivo oxidative reactions to form dehydrodiferulates. After acid and enzymatic degradation of sugar beet cell walls and fractionation of the solubilized products by hydrophobic interaction chromatography, three dehydrodiferulate-rich fractions were isolated. The structural identification of the different compounds present in these fractions was performed by electrospray-ion trap-mass spectrometry (before and after ^{18}O labeling) and high-performance anion-exchange chromatography. Several compounds contained solely Ara (terminal or α-1 → 5-linked-dimer) and dehydrodiferulate. The location of the dehydrodiferulate was assigned in some cases to the *O*-2 and in others to the *O*-5 of non-reducing Ara residues. One compound contained Gal (β-1 → 4-linked-dimer), Ara (α-1 → 5-linked-dimer) and dehydrodiferulate. The location of the dehydrodiferulate was unambiguously assigned to the *O*-2 of the non-reducing Ara residue and *O*-6 of the non-reducing Gal residue. These results provide direct evidence that pectic arabinans and galactans are covalently cross-linked (intra- or intermolecularly) through dehydrodiferulates in sugar beet cell walls. Molecular modeling was used to compute and structurally characterize the low energy conformations of the isolated compounds. Interestingly, the conformations of the dehydrodiferulate-bridged arabinan and galactan fragments selected from an energetic criterion, evidenced very nice agreement with the experimental occurrence of the dehydrodiferulated pectins. The present work combines for the first time intensive mass spectrometry data and molecular modeling to give structural relevance of a molecular cohesion between rhamnogalacturonan fragments.

Keywords: Amaranthaceae (Chenopodiaceae); Ferulic acid; Dehydrodimer; Dehydrodiferulate; Pectin; Arabinan; Galactan; Conformational minimum

1. Introduction

Plant cell walls (CW) are complex multifunctional structures constructed principally of polysaccharides. The abundance of CW bound ferulic acid (FA) is a distinctive specific feature of primary CW of species belonging to the commelinoid group of monocotyledons, the dicotyledon order Caryophyllales and all gymnosperm families (Carnachan and Harris, 2000). In species of the family Amaranthaceae (Caryophyllales) such as sugar beet (*Beta vulgaris*), spinach (*Spinacia oleracea*), glasswort (*Salicornia ramosissima*) and quinoa (*Chenopodium quinoa*), it is pectic polymers that are feruloylated (Fry, 1982; Rombouts and

Abbreviations: CID, collision-induced dissociation; CW, cell wall; CWM, cell wall material; diAra, α-1 → 5-linked dimer; diFA, dehydrodiferulate; diGal, β-1 → 4-linked dimer; ESI-IT-MS, electrospray ion-trap mass-spectrometry; EtOH, ethanol; FA, ferulic acid; hpaec, high-performance anion-exchange chromatography; *m*/*z*, mass to charge ratio; TFA, trifluoroacetic acid.

* Corresponding author. Tel.: +33 240675196; fax: +33 240675084.
E-mail address: ralet@nantes.inra.fr (M.-C. Ralet).
[1] Present address: Institut Pasteur, Unité de Biochimie Structurale, 25 rue du Dr Roux, 75724 Paris Cedex 15, France.

0031-9422/$ - see front matter © 2005 Elsevier Ltd. All rights reserved.
doi:10.1016/j.phytochem.2005.09.039

Thibault, 1986; Renard et al., 1993a, 1999). Pectin main structural features include homogalacturonic and rhamnogalacturonic regions. The latter display some Rha residues substituted by Ara- and Gal-containing side chains. FA residues are mainly ester-linked to *O*-2 of Ara residues of the main core of α-(1 → 5)-linked arabinan chains and to *O*-6 of Gal residues of the main core of β-(1 → 4)-linked type I galactan chains (Ishii and Tobita, 1993; Colquhoun et al., 1994). Recently, minor amounts of FA were assumed to be also ester-linked to *O*-5 of Ara residues of the main core of α-(1 → 5)-linked arabinan chains, indicating a potential peripheral location of some FA on pectic "hairy" regions (Levigne et al., 2004a).

The FA esters are of great interest since they can undergo in vivo oxidative coupling reactions to form dehydrodimers (diFA) (Fry, 1986). Four dimer isomers are present in cell walls (8-O-4′, 8-5′, 8-8′ and 5-5′) (Fig. 1), their relative proportion varying greatly with respect to plant origin. In most angiosperm tissues, the 8-O-4′ and 8-5′ dimers are the most abundant (Wende et al., 2000). In vivo diFA formation enables covalent cross-linking of the polysaccharides they esterify. Such coupling, that was up to recently thought to take place exclusively in the CW, was claimed to have a "tightening" effect (contribution to wall assembly, promotion of tissue cohesion, restriction of cell expansion, resistance against fungal penetration etc...) (Fry, 1986; Kamisaka et al., 1990; Ralph and Helm, 1993; Brady and Fry, 1997). It was, however, lately shown that feruloyl coupling occurred not only in the CW but also intra-protoplasmically, most likely in the Golgi apparatus (Fry et al., 2000; Obel et al., 2003). More balanced hypotheses were then proposed about the physiological role of such oxidative coupling (Fry et al., 2000). In young maize (*Zea mays* L.) cultures, much oxidative coupling of feruloyl arabinoxylans was shown to occur intra-protoplasmically. The majority of the arabinoxylan secreted onto the inner surface of the CW was assumed to be present as a pre-cross-linked coagulum that could prevent the newly deposited cellulose microfibrils to assemble through hydrogen bonds and help in that way to maintain a high CW extensibility. Older maize cultures oxidatively coupled substantially fewer of their feruloyl residues intraprotoplasmically. The intense extraprotoplasmic coupling of feruloyl arabinoxylans would here tighten the CW (Fry et al., 2000). Additionally, Obel et al. (2003) demonstrated that intracellular dimer formation is confined to specific dimers. 8-5′ diFA is indeed formed intracellularly while 5-5′ and 8-O-4′ diFA are supposed to be formed extracellularly.

Fragments composed of a pair of xylan-related oligosaccharides bridged by a 5-5′ diFA group were isolated from monocotyledons (Ishii, 1991; Saulnier et al., 1999). These fragments are likely to represent inter-polysaccharide cross-links, although the existence of intra-polysaccharide loops cannot be precluded. DiFA have been identified and quantified in sugar beet CW, where 15% to over 20% of the quantified alkali-soluble wall-bound phenolics comprised diFA, indicating a potentially high degree of polymer cross-linking (Micard et al., 1997; Waldron et al., 1997). We describe here the isolation of several diFA-bridged oligosaccharides. The structural identification of these compounds by high-performance anion-exchange chromatography (hpaec) and electrospray ion-trap mass-spectrometry (ESI-IT-MS) provides direct evidence for covalent (intra- or inter-molecular) cross-linking of pectic arabinans and galactans through diFA bridges in sugar beet CW. In an effort to supply high definition of the molecular structures of the identified diFA-bridged arabinan and galactan fragments, we computed and characterized their low energy conformations using molecular modeling techniques. The structures issued from the conformational study constitute a step forward towards a molecular comprehension of occurence, flexibility and strength of the diFA bridging effect in the CW.

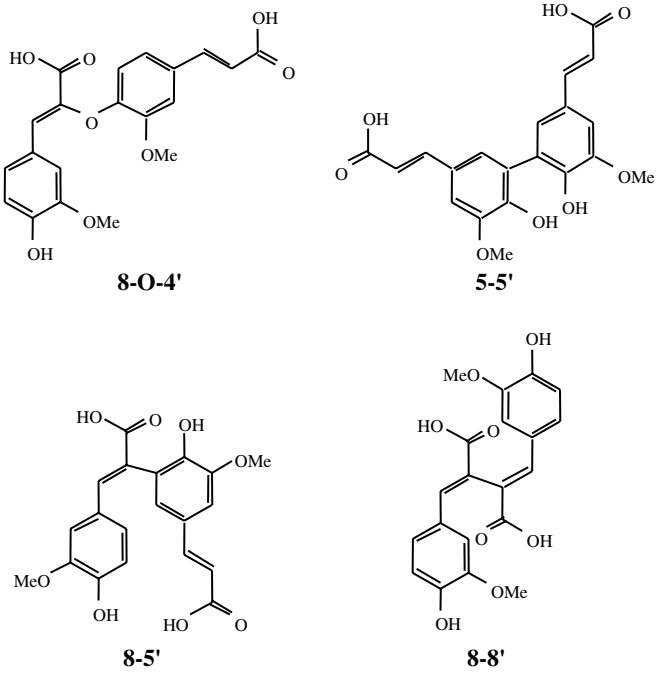

Fig. 1. Structure of the main diFA isomers present in plant cell walls.

2. Results

2.1. Isolation and chemical analysis of diFA-rich fractions

A sequential isolation process including acid and enzymatic hydrolyses and low pressure hydrophobic interaction chromatographic fractionations was followed (Fig. 2). Sugar beet root cell wall material (CWM) (FA 8.2 mg/g; diFA 0.65 mg/g) was hydrolyzed by trifluoroacetic acid (TFA) and the resulting TFA-soluble fraction precipitated by ethanol (EtOH). It was established in a previous work that such conditions allowed the recovery of most of the Ara residues in the EtOH-soluble fraction (Ralet et al.,

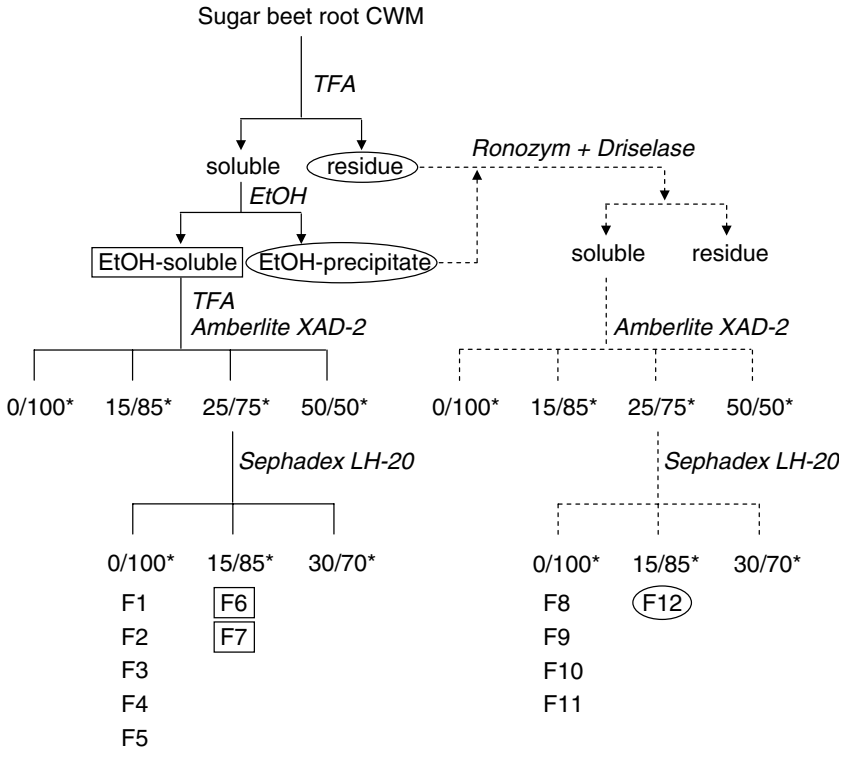

Fig. 2. Isolation of diFA-rich fractions (F6, F7 and F12) implementing acid and enzymatic hydrolyses and low pressure hydrophobic interaction chromatographic fractionations (Amberlite XAD-2 and Sephadex LH-20). ★ EtOH/water (v/v).

1994). Indeed, ~92% of the Ara residues were recovered in the EtOH-soluble fraction together with ~20% of the Gal residues and ~55% of the FA and diFA. The repartition of the different diFA isomers was similar within the EtOH-soluble fraction, EtOH-precipitate and TFA hydrolysis residue and was representative of the repartition within the initial CWM (5-5′:8-O-4′:8-5′ 4:48:48, w/w/w).

The EtOH-soluble fraction was further hydrolyzed with TFA, and loaded onto an Amberlite XAD-2 column eluted successively with water, EtOH:water 15:85 (v/v), EtOH:-water 25:75 (v/v) and EtOH:water 50:50 (v/v). Chromatographic yields were >95% for individual sugars, FA and diFA. The water-eluted fraction contained most of the total recovered sugars (97% w/w) and low amounts of FA and diFA (~1% w/w of the total recovered FA and diFA). Most of the FA and diFA (67% and 77% w/w of the total recovered FA and diFA, respectively) were present in the EtOH:water 25:75-eluted fraction that was subjected to further purification on Sephadex LH-20 eluted successively by water, EtOH:water 15:85 (v/v) and EtOH:-water 30:70 (v/v). Five fractions (F1–F5) were eluted by water and two fractions were eluted by EtOH:water 15:85 (F6, F7). The sugar and phenolic composition of each fraction are reported in Table 1. The chromatographic yields were close to 100% for individual sugars and FA and ~60% for diFA. Most of the diFA was recovered in F2, F6 and F7. F2 contained large amounts of FA (FA/diFA mol/mol of 0.96) and was not further studied. F6 and F7 contained Ara as sole sugar and low amounts of FA (FA/diFA mol/mol of 0.33 and 0 for F6 and F7, respectively). The diFA isomers repartition showed the predominance of 8-O-4′ dimer in F6 and the presence of both 5-5′ and 8-O-4′ dimers in F7. Those two fractions were selected for further study.

The EtOH-precipitate and TFA hydrolysis residue still contained altogether 80% of the Gal, 8% of the Ara and 45% of the FA and diFA initially present in the CWM. In order to recover additional diFA-bridged oligosaccharides, the EtOH-precipitate and the TFA hydrolysis residue were hydrolyzed by a mixture of Driselase® and Ronozym® two preparations rich in pectolytic activities. The resulting soluble fraction was loaded onto an Amberlite XAD-2 column as described above. Chromatographic yields were >95% for individual sugars, FA and diFA. The water-eluted fraction contained most of the total recovered sugars (95% w/w) and low amounts of FA and diFA (2.3% and 7.5% w/w of the total recovered FA and diFA, respectively). Most of the phenolics (71% and 60% w/w of the total recovered FA and diFA, respectively) were present in the EtOH:water 25:75-eluted fraction. Unlike Driselase®, Ronozym® contains some ferulate esterase activity and 35% of the FA recovered consisted of free FA. Interestingly, this ferulate esterase was similarly active on diFA as 32% of the diFA recovered consisted of free diFA. The EtOH:water 25:75-eluted fraction, that contained the major part of diFA, was subjected to further purification on Sephadex LH-20 after removal of free FA and diFA by ether extraction at pH 2. The ether extract

Table 1
Composition of the Sephadex LH-20 fractions

Fractions	% of total amount eluted from LH-20			Sugar repartition within each fraction (mol%)				diFA repartition within each fraction (mol%)			FA*100/diFA	(Ara + Gal)/(FA + diFA)
	Sugars	FA	DiFA	GalUA	Rha	Ara	Gal	5-5′	8-O-4′	8-5′	(mol%)	(mol/mol)
TFA												
F1	13	1	2	39	16	11	34	9	52	39	92	12
F2	25	13	21	0	1	64	35	8	68	24	96	3
F3	20	20	7	0	0	100	0	45	17	38	99	2
F4	39	65	9	0	0	100	0	6	41	53	>99	1
F5	1	1	6	0	0	96	0	5	32	62	85	2
F6	1	<1	34	0	0	100	0	4	78	19	33	2
F7	1	0	22	0	0	100	0	41	55	5	0	3
Enzymes												
F8	47	8	44	0	13	17	34	11	36	53	85	11
F9	9	11	13	0	1	10	74	12	46	43	96	3
F10	42	77	24	0	0	3	97	8	32	61	99	2
F11	2	4	8	0	0	65	35	9	73	18	94	2
F12	<1	0	11	0	0	45	55	79	21	0	20	2

did not contain any sugar. Four fractions (F8–F11) were eluted by water and one fraction was eluted by EtOH:water 15:85 (F12). The sugar and phenolic composition of each fraction are reported in Table 1. The chromatographic yields were close to 100% for individual sugars, FA and diFA. Most of the diFA was recovered in F8, showing that diFA were still attached to sugar moieties of high degree of polymerization. F9–F11 also contained substantial amounts of diFA but contained also large amounts of FA (FA/diFA mol/mol of 0.96, 0.99 and 0.94 for F9, F10 and F11, respectively) and were not further studied. F12 contained substantial amounts of diFA, Ara and Gal in similar quantities and was lowly contaminated by FA (FA/diFA mol/mol of 0.20). The diFA isomers repartition showed the predominance of the 5-5′ dimer in F12. This fraction was selected for further study.

2.2. hpaec and MS characterization of diFA-rich fractions

F6, F7 and F12 were analyzed by hpaec at pH 13 (Fig. 3). The ester bond FA residues are released due to the strongly alkaline conditions used and pure carbohydrates are separated on the column. By comparison with α-(1 → 5)-arabinan- and β-(1 → 4)-galactan-derived oligosaccharides, it was shown that F6 and F7 contained solely Ara monomers and α-(1 → 5)-linked Ara dimers and that F12 contained α-(1 → 5)-linked Ara dimers and β-(1 → 4)-linked Gal dimers. F6, F7 and F12 were further analyzed by negative ESI-IT-MS by direct infusion into the electrospray source (Fig. 4). Several compounds were detected in F6 with deprotonated singly charged $[M - H]^-$ ions at mass-to-charge ratio (*m/z*) 517, 649, 781 and 913, that could correspond to Ara_1-diFA, Ara_2-diFA, Ara_3-diFA and Ara_4-diFA, respectively; deprotonated $[M - H]^-$ ions at *m/z* 473, 499, 817 and 1081, that could correspond to decarboxylated Ara_1-diFA, dehydrated Ara_1-diFA, Ara_3-diFA + $2H_2O$ and Ara_5-diFA + $2H_2O$, respectively; deprotonated cluster $[2M - H]^-$ ions at *m/z* 1299, that could correspond to Ara_2-diFA. Major ions at *m/z* 649 (compound **1**), 781 (compound **2**) and 913 (compound **3**) were chosen

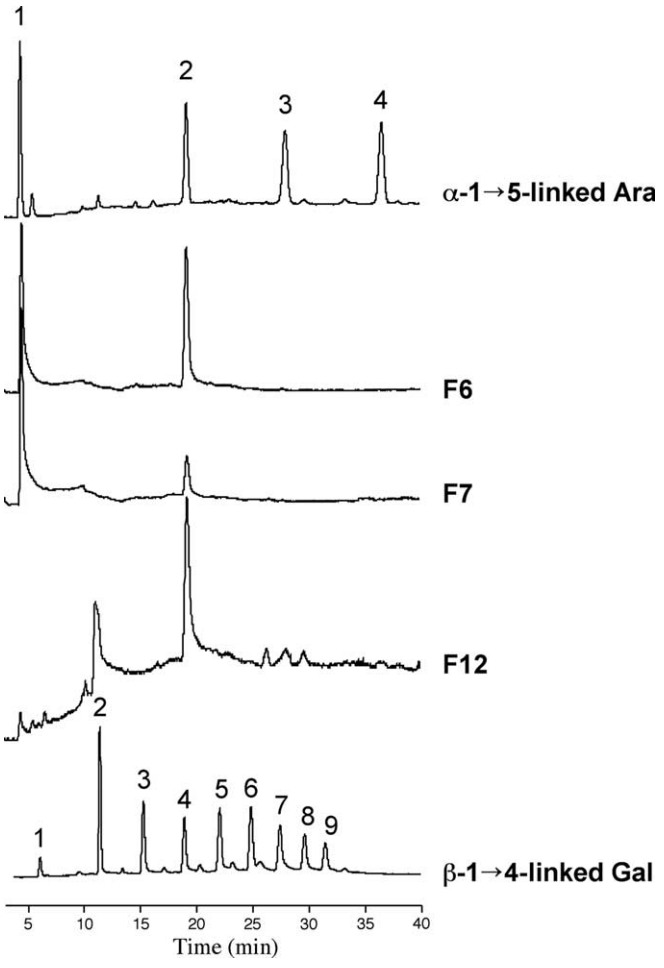

Fig. 3. High performance anion exchange chromatography (pH 13) profiles of the diFA-rich fractions (F6, F7 and F12). α-(1 → 5)-linked-arabinan-derived oligosaccharides and β-(1 → 4)-linked-galactan-derived oligosaccharides were used as standards.

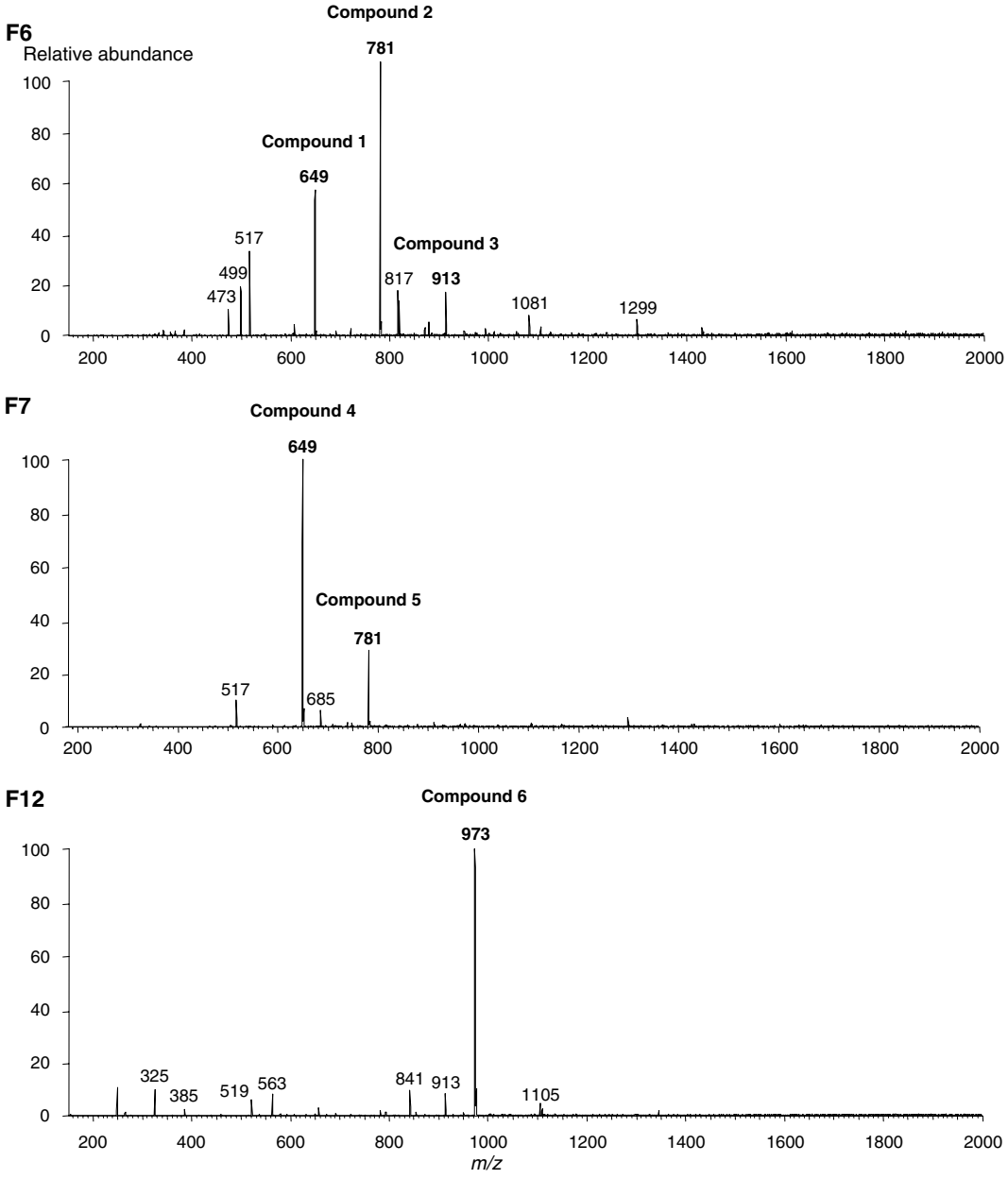

Fig. 4. Negative full MS spectra of the diFA-rich fractions (F6, F7 and F12).

for further structural studies. F7 exhibited two main signals with deprotonated $[M - H]^-$ ions at *m/z* 649 (compound **4**) and 781 (compound **5**) that could correspond to Ara_2-diFA and Ara_3-diFA. Finally, a prominent ion at *m/z* 973 (compound **6**) that could correspond to Ara_2-Gal_2-diFA, was detected in F12. After ^{18}O-labeling of the whole fractions, compounds **2**–**6** gained 4 mass units, in agreement with the presence of two reducing ends while compound **1** gained 2 mass units, in agreement with the presence of one reducing end. Considering the results obtained, the following partial structure could be assigned to the different compounds:

Compound **1**	*m/z* 649	diFA-Ara-α-(1 → 5) Ara
Compound **2**	*m/z* 781	Ara-diFA-Ara-α-(1 → 5) Ara
Compound **3**	*m/z* 913	Ara (5 ← 1)-α-Ara-diFA-Ara-α-(1 → 5) Ara
Compound **4**	*m/z* 649	Ara-diFA-Ara
Compound **5**	*m/z* 781	Ara-diFA-Ara-α-(1 → 5) Ara
Compound **6**	*m/z* 973	Gal (4 ← 1)-β-Gal-diFA-Ara-α-(1 → 5) Ara

2.3. Full structural assignment by MS fragmentation techniques

MS^n experiments were carried out in order to allow the precise location of the phenolic moieties onto the sugar rings for the different compounds. MS^n experiments were performed by negative ESI-IT-MS by direct infusion of F6, F7 and F12 into the electrospray source. The electrospray ionization followed by formation of fragment ions by collision-induced dissociation (CID) allows sensitive

mapping and sequencing of oligosaccharides. Carbohydrates undergo two types of fragmentation: those of glycosidic cleavages and those of cross-ring fragmentation. According to the cross-ring fragmentation, linkage and branching patterns can be established (Vakhrushev et al., 2004). For sequencing, glycosidic cleavages along the chain are major tools, especially after ^{18}O labelling of the reducing end. In the present work, ^{18}O labeling was particularly useful for establishing whether the losses forming ions contained two (**), one (*), or no ^{18}O-labeled reducing end.

2.3.1. Compounds arising from F6

Compounds **1**, **2** and **3** exhibited very similar fragmentation patterns and the spectra obtained for compound **3** will be the ones fully presented here (Fig. 5). Fig. 6 shows the different cleavages observed at each MS step.

After isolation and collision-induced dissociation (CID) of the parent ion at *m/z* 913 (Ara-Ara-diFA-Ara-Ara) in an MS^2 analysis, a series of fragment ions appeared (Fig. 5(a)). The prominent ions produced at *m/z* 853 and 823, corresponding to losses of 60 Da ($C_2H_4O_2$) and 90 Da ($C_3H_6O_3$), respectively, resulted from cross ring cleavages. A glycosidic fragment ion at *m/z* 781 (132 Da loss), corresponding to the loss of one Ara unit, was produced. After isolation and CID of the doubly labeled parent ion at *m/z* 917**(*Ara-Ara-diFA-Ara-Ara*), a series of singly labeled prominent fragment ions appeared at *m/z* 783*, 825*, and 855*, corresponding to losses of 134 Da (labeled Ara unit), 92 Da (labeled $C_3H_6O_3$), and 62 Da (labeled $C_2H_4O_2$), respectively (Fig. 5(a) inset). The fragmentation pattern observed for labeled and non-labeled compound **3** is consistent with a linkage through *O*-5 of one of the two reducing Ara residues (Harvey, 2000; Quéméner and Ralet, 2004; Levigne et al., 2004b) (arbitrarily quoted Ara1 on Fig. 6), in agreement with hpaec data. The fragment ion at *m/z* 781 undergoes further fragmentations that were assigned to H_2O loss (*m/z* 763) and to cross-ring cleavage fragment ions (*m/z* 721 and 691, respectively). The ion at *m/z* 649 corresponds to the loss of one extra Ara residue (132 Da loss). The peak at *m/z* 631 could be assigned to the loss of a water molecule from the ion at *m/z* 649. The ^{18}O-labeled ion at 783* also undergoes further fragmentations and one can differentiate between the loss of the second reducing labeled Ara residue (*m/z* 649, 134 Da loss, Ara4 in Fig. 6) and the loss of a non labeled Ara residue in ester linkage with the phenolic moiety (*m/z* 651*, 132 Da loss, Ara2 in Fig. 6). The peak at *m/z* 633* could be assigned to the loss of a non-labeled water molecule (18 Da loss) from the ion at *m/z* 651*.

The glycosidic cleavage ion at *m/z* 781 (Ara-Ara-diFA-Ara↵) was selected for further fragmentation in a MS^3 CID experiment (*m/z* 913 > 781 > products) (Figs. 5(b), 6(b)). The MS^3 trace provided the four fragment ions at *m/z* 763, 721, 691 and 649 that were already observed in MS^2 analysis. The MS^3 CID experiment conducted on the ^{18}O-labeled ion at 783* (*Ara-Ara-diFA-Ara↵) (*m/z* 917** > 783* > products) revealed to be much more informative (Fig. 5(b), inset) with a clear differentiation between fragments arising from the second reducing labeled Ara residue (Ara4 in Fig. 6) and the loss of a non labeled Ara residue in ester linkage with the phenolic moiety (Ara2 in Fig. 6). Besides glycosidic fragment ions at *m/z* 649 and 651* and consecutive water losses at 631 and 633*, two cross ring cleavage fragment ions at *m/z* 721 and 691, involving the labeled Ara residue, and one cross ring cleavage fragment ion at *m/z* 723*, involving the non labeled Ara residue, were observed. The fragmentation pattern observed for the labeled Ara residue (62 and 92 Da losses) is again consistent with a linkage through *O*-5 of this reducing Ara residue (Ara4 in Fig. 5), in agreement with hpaec data. The fragmentation observed for the non-labeled Ara residue (Ara2 in Fig. 6) was interpreted by comparison with CID product-ion patterns obtained for feruloylated arabinose containing mono- and disaccharides with known linkage configurations (Quéméner and Ralet, 2004). Indeed, the CID spectrum of an Ara residue substituted on *O*-2 by a FA residue was shown to be dominated by a diagnostic cross-ring cleavage ion at (−108 Da) and an intense water loss, while a high relative abundance of the diagnostic cross-ring cleavage ion at (−60 Da) together with moderate water loss were characteristic of linkage of FA through the *O*-5 of the Ara unit. The fragmentation observed for the non-labeled Ara residue in ester linkage with the phenolic moiety, namely the abundant production of the ion at *m/z* 723* (60 Da loss), the absence of 108 Da loss and the absence of water loss, is consistent with the linkage of the phenolic moiety through the *O*-5 of the Ara unit.

The fragment ions at *m/z* 649 or *m/z* 651* were not produced in sufficient quantity (either from MS^2 or MS^3 analyses) to allow further fragmentation. MS^3 analysis of the intense ion at *m/z* 631 (*m/z* 913 > 631 > products) was tentatively performed (Figs. 5(c) and 6(c)). This ion was shown to arise solely from the loss of two consecutive Ara units (one labeled and one non labeled, quoted Ara1 and Ara2 in Fig. 6, respectively) (Ara-Ara-diFA↵H_2O) (Figs. 5(b) and 6(b)). Beside moderate water loss (*m/z* 613), prominent ions produced at *m/z* 571 and 541, corresponding to losses of 60 and 90 Da, respectively, resulted from cross-ring cleavages. A glycosidic fragment ion at *m/z* 499 (loss 132 Da), corresponding to the loss of one Ara unit (Ara4 in Fig. 6), was produced. This fragmentation pattern confirms the linkage through *O*-5 of this reducing Ara residue.

MS^4 analysis of the glycosidic fragment ion at *m/z* 499 (↳Ara-diFA↵H_2O) (*m/z* 913 > 631 > 499 > products) was performed (Figs. 5(d) and 6(d)). The fragmentation observed for this last Ara residue (Ara3 in Fig. 6), namely the abundant production of the ion at *m/z* 439 (60 Da loss), the absence of 108 Da loss and the absence of water loss, is again consistent with the linkage of the phenolic moiety through the *O*-5 of this last Ara unit (Quéméner and Ralet, 2004).

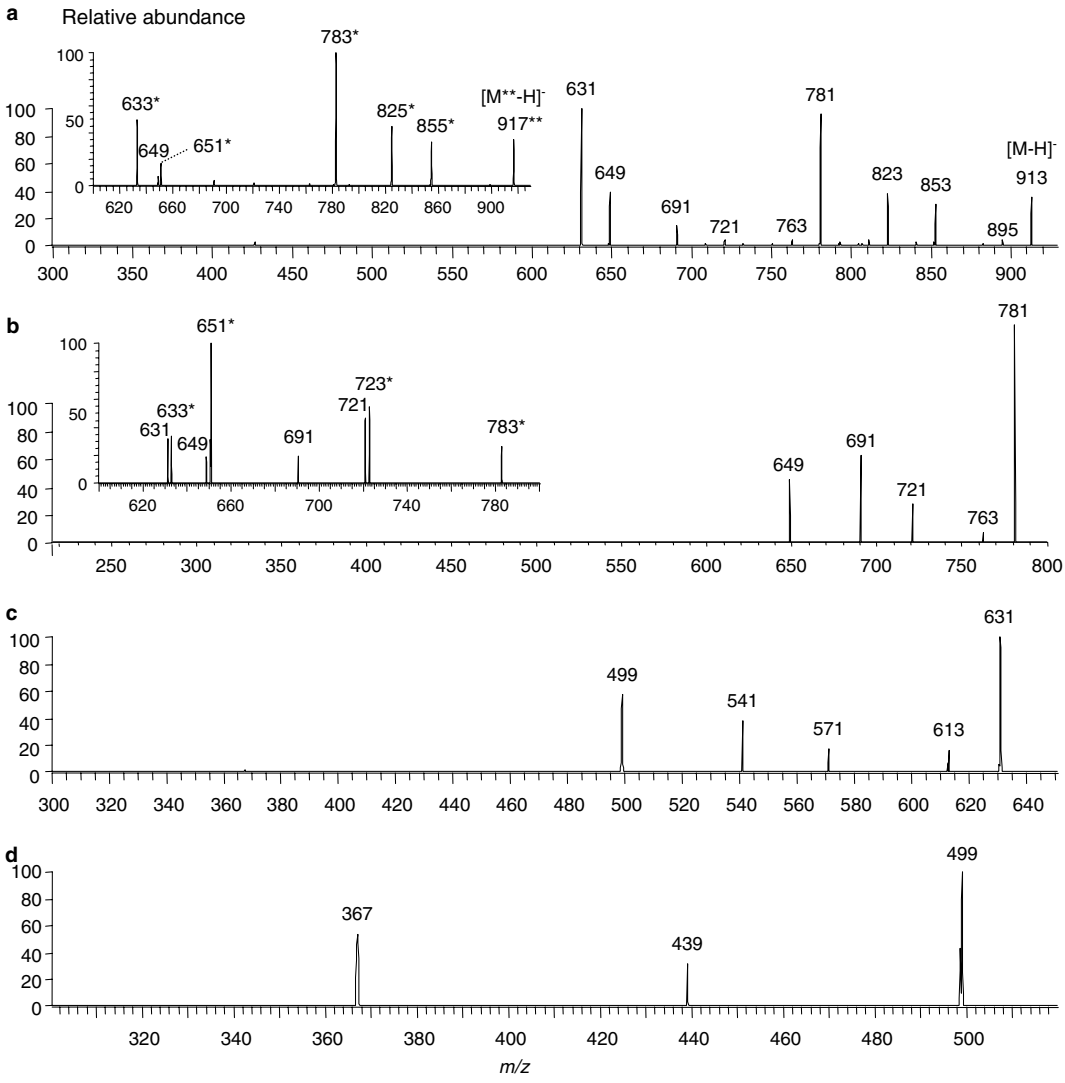

Fig. 5. Negative MS^n experiment spectra of compound 3 (Ara-Ara-diFA-Ara-Ara) arising from F6. (a) MS^2 experiment (m/z 913 > products), inset: MS^2 experiment of ^{18}O-labeled compound (m/z 917** > products); (b) MS^3 experiment (m/z 913 > 781 > products), inset: MS^3 experiment of ^{18}O-labeled compound (m/z 917** > 783* > products); (c) MS^3 experiment (m/z 913 > 631 > products); (d) MS^4 experiment (m/z 913 > 631 > 499 > products).

Considering the results obtained, the following structures could be assigned to the main compounds present in F6:

Compound **1** diFA → 5-Ara-α-(1 → 5) Ara
Compound **2** Ara-(5 ← diFA → 5)-Ara-α-(1 → 5) Ara
Compound **3** Ara (5 ← 1)-α-Ara-(5 ← diFA → 5)-Ara-α-(1 → 5) Ara

The 8-O-4′ diFA isomer was largely predominant in F6.

2.3.2. Compounds arising from F7

After isolation and CID of the doubly labeled parent ion at m/z 785** (*Ara-diFA-Ara-Ara*, compound **5**), a series of singly labeled prominent fragment ions appeared. The spectrum was difficult to interpret as both reducing ends generated fragment ions. Therefore, some fragment ions were diagnostic of a linkage through *O*-5 of one of the two reducing Ara residues while others were characteristic of a reducing Ara residue substituted on *O*-2 by a phenolic moiety (Quéméner and Ralet, 2004). We assumed, considering the fragment ions produced and the hpaec data, that the reducing Ara residue in ester linkage with the phenolic moiety is mainly linked through *O*-2 although the presence of minor amounts of *O*-5 linkage cannot be totally precluded. This was confirmed by the MS^4 analysis of the glycosidic fragment ion at m/z 517 (↳diFA-Ara↵) (m/z 785** > 651* > 517 > products). Indeed, the fragmentation observed for the Ara residue, namely the abundant production of the ion at m/z 409 (108 Da loss), the absence of 60 Da loss and the abundance of water loss, was consistent with the linkage of the phenolic moiety through the *O*-2 of this Ara unit (Quéméner and Ralet, 2004).

Similarly, compound **4** (Ara-diFA-Ara) exhibited MS^2 and MS^3 fragmentation patterns that were dominated by 108 Da loss fragment ions (base peaks) and water loss assessing the linkage of the phenolic moiety through the *O*-2 of Ara residues at each side (Quéméner and Ralet, 2004).

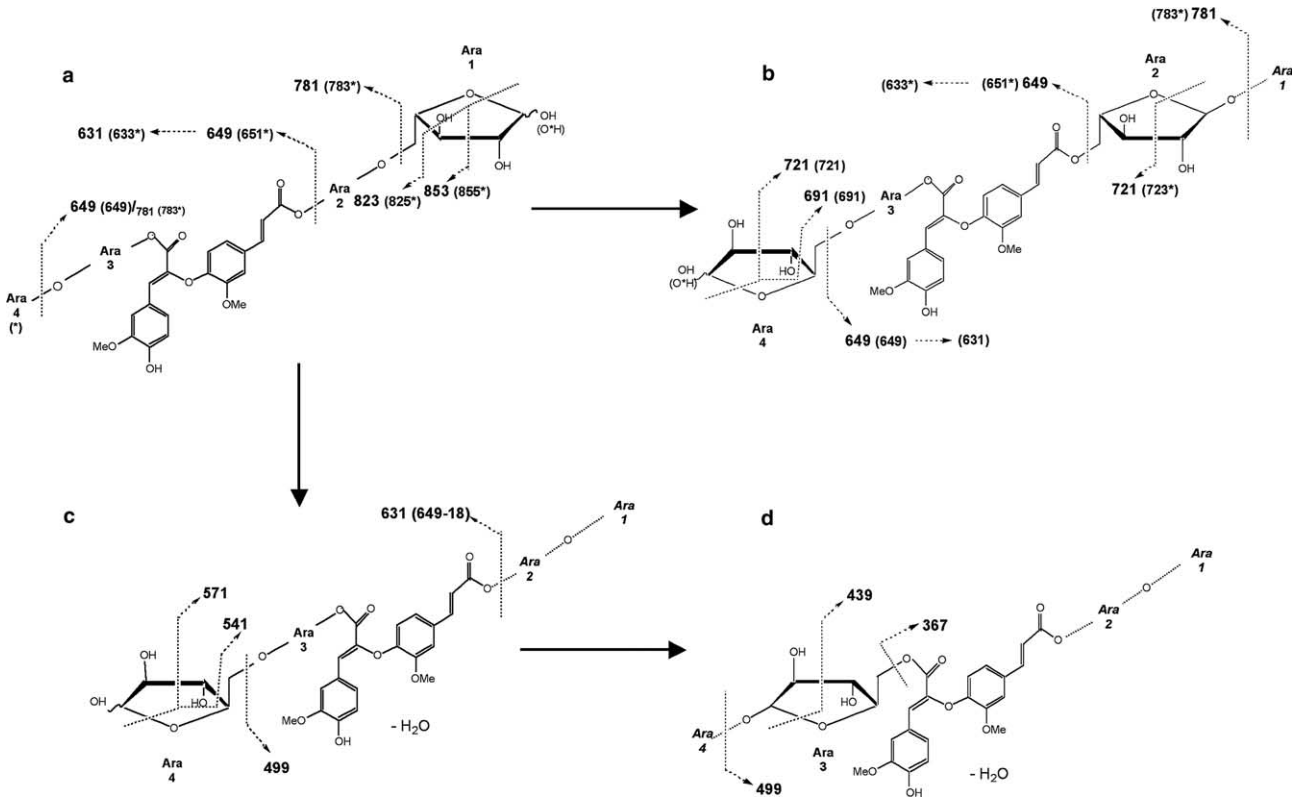

Fig. 6. Proposed structure of compound **3** (Ara-Ara-diFA-Ara-Ara) arising from F6 and observed cleavages at each MS step. (a) MS^2 experiment (*m/z* 913 > products and *m/z* 917** > products); (b) MS^3 experiment (*m/z* 913 > 781 > products and *m/z* 917** > 783* > products); (c) MS^3 experiment (*m/z* 913 > 631 > products); (d) MS^4 experiment (*m/z* 913 > 631 > 499 > products).

Considering the results obtained (supplemental data online 1 and 2), the following structures could be assigned to the main compounds present in F7:

Compound **4** Ara-(2 ← diFA → 2)-Ara
Compound **5** Ara-(2 ← diFA → 2)-Ara-α-(1 → 5) Ara

5-5′ and 8-O-4′ diFA isomers were present in roughly similar amounts in F7.

2.3.3. Compounds arising from F12

MS^2 to MS^5 CID experiments of the parent ion at *m/z* 973 (Gal-Gal-diFA-Ara-Ara) or of the doubly labeled parent ion at *m/z* 977** (*Gal-Gal-diFA-Ara- Ara*) provided evidence for a 1 → 4 linkage between the two Gal residues and for a 1 → 5 linkage between the two Ara residues, in agreement with hpaec data. The fragmentation pattern observed for the Gal residue in ester linkage with the phenolic moiety (prominent 60 Da loss, 90 and 120 Da losses) demonstrated that the non-reducing Gal unit is linked through *O*-6 to the phenolic moiety (Quéméner and Ralet, 2004). The fragmentation pattern observed for the Ara residue in ester linkage with the phenolic moiety, namely the abundant 108 Da loss, the absence of 60 Da loss and the abundance of water loss, assessed the linkage of the phenolic moiety through the *O*-2 of this Ara unit (Quéméner and Ralet, 2004).

Considering the results obtained (supplemental data online 3 and 4), the following structure could be assigned to the main compound present in F12:

Compound **6** Gal (4 ← 1)-β-Gal-(6 ← diFA → 2)-Ara-α-(1 → 5) Ara.

The 5-5′ diFA isomer was largely predominant in F12.

2.4. Molecular modeling

With respect to the type of diFA, the nature of the sugar moieties and the linkage position of the phenolic moieties to the sugar rings, four main types of diFA-bridged pectic oligosaccharides were evidenced:

Ara(5 ← 1)-α-Ara-(5 ← 8-O-4′ → 5)-Ara-α-(1 → 5)Ara.
Ara(5 ← 1)-α-Ara-(2 ← 8-O-4′ → 2)-Ara-α-(1 → 5)Ara.
Ara (5 ← 1)-α-Ara-(2 ← 5-5′ → 2)-Ara-α-(1 → 5) Ara.
Gal (4 ← 1)-β-Gal-(6 ← 5-5′ → 2)-Ara-α-(1 → 5) Ara.

The prerequisite for building and understanding the structure of these diFA-bridged oligosaccharides was a preliminary description of their constitutive disaccharide and diFA components, namely α-L-Ara*f*-(1 → 5)-L-Ara*f*, β-D-Gal*p*-(1 → 4)-D-Gal*p*, 8-O-4′ and 5-5′. Their main conformational features are listed in Table 2.

2.4.1. Conformation of L-Araf-5 ← 1-α-L-Araf-(5 ← 8-O-4′ → 5)-L-Araf-α-(1 → 5)-L-Araf

The two conformations that displayed the lowest energy were selected among the numerous probable geometries (Figs. 7A and A′). The conformation (A) did not show the diFA in the stacking conformation but on the contrary rather extended. The second minimum (A′) displayed the stacking interaction. Conformation (A′) was the one with the lowest energy compared to other compounds. This minimum served as a reference and its energy value was arbitrarily zeroed to highlight later the energy discrepancies of its counterparts. The dihedral angles for the first junction were, respectively, C_3–C_4–C_5–O_{10} at −92°, C_4–C_5–O_{10}–C_9 at −102° and O_{10}–C_9–C_8–$O_{4\prime}$ at −176° and the ones for the second junction were $C_{1\prime}$–$C_{7\prime}$–$C_{8\prime}$–$C_{9\prime}$ at −83°, $C_{7\prime}$–$C_{8\prime}$–$C_{9\prime}$–$O_{10\prime}$ at −178° and $C_{8\prime}$–$C_{9\prime}$–$O_{10\prime}$–C_5^* at −175°.

2.4.2. Conformation of L-Araf-(5 ← 1)-α-L-Araf-(2 ← 8-O-4′ → 2)−L-Araf-α-(1 → 5)−L-Araf

The two conformations that displayed the lowest energy were selected among the numerous probable geometries. In those cases, the diAra and the 8-O-4′ diFA moieties adopted their intrinsic low energy conformation. Markedly, the diFA moiety displayed a quite compact conformation allowed by the π stacking interaction. The difference between the two conformations came from the dihedral angles of the junction between the two entities that showed two distinct positions after minimization. The energy delta was 5.5 kcal/mol. The conformation that led to the lowest energy is illustrated in Fig. 7B. This was by far the most compact conformation among the different compounds. The dihedrals of the first junction were, respectively, C_3–C_2–O_{10}–C_9 at +38°, C_2–O_{10}–C_9–C_8 at −165°, O_{10}–C_9–C_8–$O_{4\prime}$ at −26° and C_9–C_8–$O_{4\prime}$–$C_{4\prime}$ at +133° and the ones for the second junction were $C_{1\prime}$–$C_{7\prime}$–$C_{8\prime}$–$C_{9\prime}$ at +174°, $C_{7\prime}$–$C_{8\prime}$–$C_{9\prime}$–$O_{10\prime}$ at +38°, $C_{8\prime}$–$C_{9\prime}$–$O_{10\prime}$–C_2^* at −153° and $C_{9\prime}$–$O_{10\prime}$–C_2^*–C_3^* at −153°.

2.4.3. Conformation of L-Araf-(5 ← 1)-α-L-Araf-(2 ← 5-5′ → 2)−L-Araf-α-(1 → 5)−L-Araf

The lowest energy conformation found for that compound showed the diFA moiety slightly tilted and the two diAra moieties in the minA configuration. The dihedral angles for the first junction were, respectively, C_3–C_2–O_{10}–C_9 at −156°, C_2–O_{10}–C_9–C_8 at −165° and O_{10}–C_9–C_8–C_7 at −25° and C_9–C_8–C_7–C_1 at +133°. The dihedral angles for the second junction were $C_{1\prime}$–$C_{7\prime}$–$C_{8\prime}$–$C_{9\prime}$ at +174°, $C_{7\prime}$–$C_{8\prime}$–$C_{9\prime}$–$O_{10\prime}$ at +37°, $C_{8\prime}$–$C_{9\prime}$–$O_{10\prime}$–C_2^* at −153° and $C_{9\prime}$–$O_{10\prime}$–C_2^*–C_3^* at −153° (Fig. 7C). The energy value was, respectively, 17.4 kcal/mol above the reference, where the diFA was 8-O-4′ linked.

2.4.4. Conformation of D-Galp-(4 ← 1)-β-D-Galp-(6 ← 5-5′ → 2)-L-Araf-α-(1 → 5)-L-Araf

Two low energy conformations were found for that compound , one of them being illustrated on Fig. 7D. The 5-5′ diFA was tilted and both the diAra and diGal adopted one more time their lowest energy configuration. The dihedral angles of the first junction were, respectively, C_3–C_2–O_{10}–C_9 at −162°, C_2–O_{10}–C_9–C_8 at −177° and O_{10}–C_9–C_8–C_7 at +4°. The dihedral angles of the second junction were $C_{8\prime}$–$C_{9\prime}$–$O_{10\prime}$–C_6^* at −165°, $C_{9\prime}$–$O_{10\prime}$–C_6^*–C_5^* at +165° and $O_{10\prime}$–C_6^*–C_5^*–C_4^* at +55°.

Computation with the CVFF force field evidenced weak energy discrepancy between all the conformers of a given compound. Each oligosaccharide moiety, especially the

Table 2
Main conformational features of the constitutive disaccharides (diAra and diGal) and diFA components

α-L-Ara*f*-(1 → 5)-L-Ara*f*		Hydrogen bondings
Two minima		
Min A −72°; −178°; −158°	Extended TG conformation	$O_2 \cdots O_{3\prime}$
Min B −159°; −176°; +180°	Very extended TG conformation	$O_{3\prime} \cdots O_{5\prime}$
Results relevant with Cros et al. (1993, 1994) and Janaswami and Chandrasekaran (2005)		
Supplementary data online 5A		
β-D-Gal*p*-(1 → 4)-D-Gal*p*		
One large minimum		
Min −80°; +128°		$O_4 \cdots O_6$
		$O \cdots O_{6\prime}$
Supplementary data online 5B		
8-O-4′ diFA		
Two minima		
Min with π stacking	Compact geometry	$O_{11} \cdots O_{3\prime}$
Min without π stacking	Stretched orientation	None
Supplementary data online 6A		
5-5′ diFA		
Four minima		
Min A − 136°	All the conformations are energetically comparable	
Min B + 46°		$O_4 \cdots O_{4\prime}$
Min C + 136°		$O_4 \cdots C_{5\prime}$
Min D − 53°		
Supplementary data online 6B		

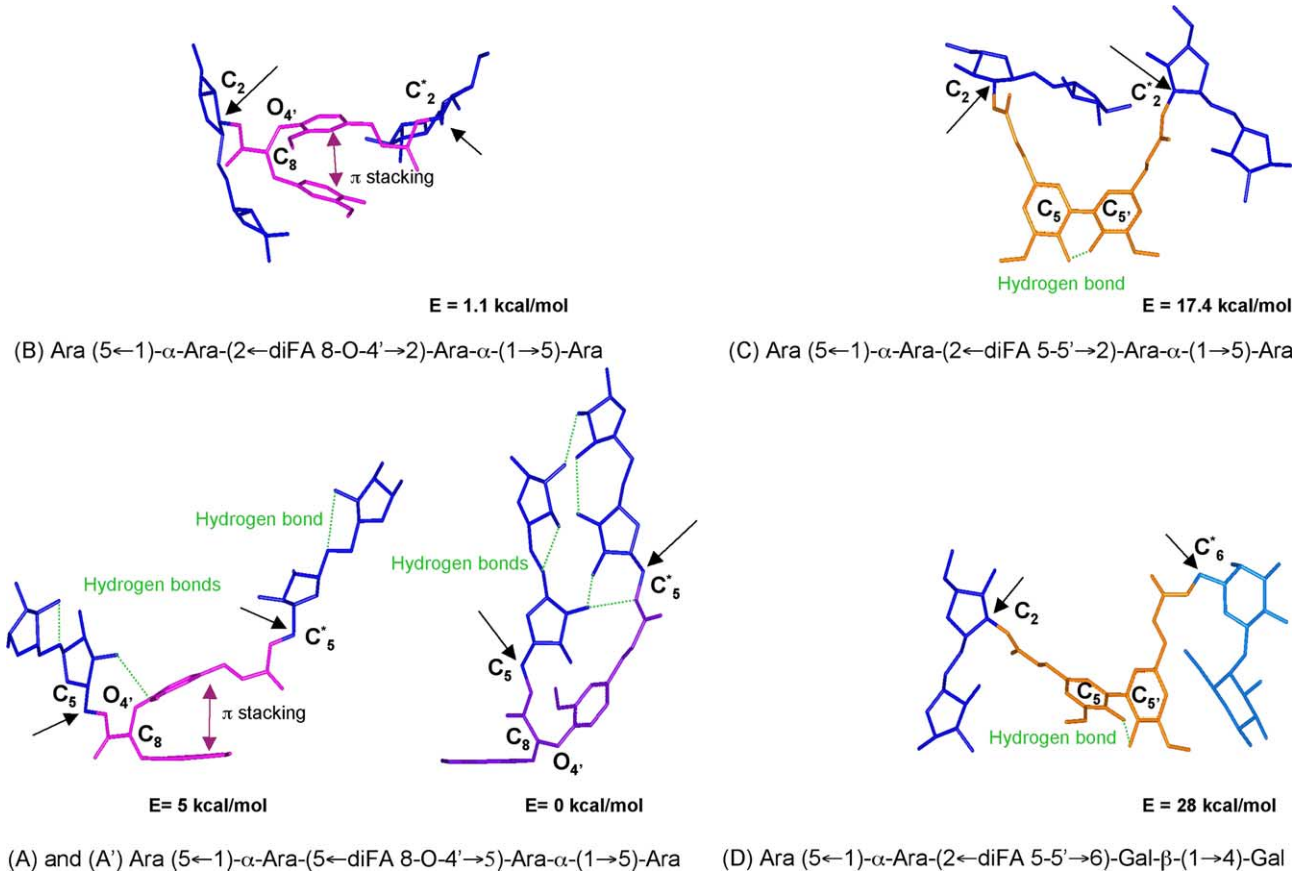

Fig. 7. Best conformers for each diFA-bridged oligosaccharides. The conformations display compact to extended conformations, combining either strong stacking (B), extensive hydrogen bonding (A′ and C), both (A) or none (D). Black arrows evidence the junction between the disaccharide and the diFA; dotted lines in green show the hydrogen bond network and the magenta arrow the stacking interaction.

diAra moiety, contributed for a large part to the high flexibility and to the clusterization of isoconformers. For a given compound, it was thus irrelevant to discriminate a unique geometry from its numerous and equiprobable counterparts. Since the aim of the study was everything but an extensive catalog of all the conformational possibilities of the diFA-bridged oligosaccharides, one or two of the lowest energy conformations for each compound were kept for clear illustration and structural discussion.

3. Discussion

Very few covalent cross-links between CW polymers have been conclusively identified. As mentioned by Mort (2002), cross-links do not need to be very abundant in the CW as a minimum of two cross-links per polymer molecule is sufficient to form a three-dimensional network. Ishii (1991) and Saulnier et al. (1999) succeeded in isolating and characterizing compounds containing a diFA bridging two arabinoxylan-derived oligosaccharides from monocotyledon CW, namely bamboo (*Phyllostahys edulis*) shoots and (*Zea mays*) maize bran. Saponification of sugar beet root CW yields not only FA but also several diFA (Micard et al., 1997; Waldron et al., 1997; Wende et al., 1999). In sugar beet root, around 20% of the total FA is in dimer form, the main dimers being 8-O-4′ diFA and 8-5′ diFA (Micard et al., 1997; Waldron et al., 1997). These diFA were claimed to cross-link pectic polysaccharides via the Ara-rich and possibly Gal-containing neutral side-chains (Waldron et al., 1997) to which most of the monomeric FA is esterified (Ralet et al., 1994; Colquhoun et al., 1994), although no experimental evidence supported these locations. In a previous work, we enzymatically recovered and partially characterized a diFA oligoarabinan from sugar beet root CWM but the exact location of diFA on arabinan chains could not be elucidated (Levigne et al., 2004b). In the present work, several diFA oligosaccharide diesters were isolated and their structures described. Besides these original structural assignments, conformational data for diFA moieties and diFA-bridged oligosaccharides are provided here for the first time. Two types of α-(1 → 5)-linked-arabinan-derived oligosaccharides bridged by a diFA group were recovered.

The first type represented 4% of the total diFA that was released by alkali treatment of the CWM. The phenolic moieties were found attached to Ara units on *O*-2, in agreement with the location of monomeric FA residues that are mainly ester-linked to *O*-2 of Ara residues of the main core of α-(1 → 5)-linked arabinan chains

(Ishii and Tobita, 1993; Colquhoun et al., 1994). This type displayed the 5-5′ and 8-O-4′ diFA in roughly similar amounts. The connection outline appeared completely different depending on the diFA nature (5-5′ or 8-O-4′), the conformation being sensitively more stable for the 8-O-4′ one. This is likely to be due to π stacking interaction between the two phenolic moieties. This interaction favors resonance between the π electron of the aromatic rings and can be considered as quite strong (Vyas, 1991). This feature is responsible for the subsequent orientation of the two diAra fragments. This is a unique feature, characteristic of the 8-O-4′ connection. For a 5-5′ connection, the orientation of the diFA favors a hydrogen bond between the hydroxyl groups O4-O4′of the two phenolic entities so that the diAra fragments tend to orient in the same direction and are close enough to hydrogen bond each other.

The second type represented 6.3% of the total diFA released by alkali treatment of the CWM and 8-O-4′ dimers were largely predominant. The phenolic moieties were here found attached to Ara units on *O*-5. We previously evidenced this specific location for minor amounts of monomeric FA and hypothesized a potential peripheral location for those *O*-5-linked FA on pectic ''hairy'' regions (Levigne et al., 2004a). Two low energy conformations were evidenced. For the first one, π stacking interaction between the diFA was attested, as mentioned above. Interestingly, the second low energy conformation displayed the 8-O-4′ diFA in an extended outline that favors the connection through hydrogen bonds of the two arabinan chains. Such feature, by lowering the high degree of freedom of the structure, could stabilize it and be responsible for the very low energy of this conformation.

Finally, an α-(1 → 5)-linked-arabinan-derived oligosaccharide bridged by a diferuloyl group to a β-(1 → 4)-linked-galactan-derived oligosaccharide was recovered. This compound represented 2% of the total diFA released by alkali treatment of the CWM and 5-5′ dimers were largely predominant. The phenolic moieties were found attached to Ara unit on *O*-2 and to Gal unit on *O*-6. As mentioned above, the 5-5′ diFA displayed a strong internal hydrogen bond.

Previous studies (Guillon and Thibault, 1989; Guillon et al., 1989; Oosterveld et al., 2000a, 2002) stated that sugar beet arabinans have a backbone of 60–70 (1 → 5)-linked α-L-Ara*f* units, half of which being substituted – on *O*-3 (∼90%) and on *O*-2 and *O*-3 (∼10%) – by single-unit Ara*f* and by rare short (1 → 3)-linked α-L-Ara*f* chains. Sugar beet β-(1 → 4)-linked-D-galactans revealed to be most likely almost linear and of low degree of polymerization (Guillon and Thibault, 1989). According to these structural characteristics, the diFA moieties could:

(i) connect arabinan chains via the *O*-2 of internal Ara residues from α-(1 → 5)-linked chains (5-5′ or 8-O-4′ connection),
(ii) connect arabinan chains via the *O*-5 of Ara residues, presumably at non-reducing ends of α-(1 → 5)-linked Ara chains (8-O-4′ connection),
(iii) connect arabinan and galactan chains via the *O*-2 of an internal Ara residue from an α-(1 → 5)-linked arabinan chain and the *O*-6 of an internal Gal residue from a β-(1 → 4)-linked galactan chain (5-5′ connection).

The isolation of diFA oligosaccharide diesters is however not proof of inter-pectic cross-linking as those compounds can also be generated if the diferuloyl group originally acted as an intra-pectin bridge. Arabinan side-chains are clearly long and flexible enough to allow the formation of an intra-chain diferuloyl loop without creating steric clashes between the adjacent sugar rings. Furthermore, connections could imply two individual arabinan and/or galactan chains belonging to the same pectic molecule. However, inter-polysaccharide diFA cross-links have been hypothesized by other experimental approaches on sugar beet pectins and also considered as most probable in a previous computational modelling study on grass heteroxylans (Hatfield and Ralph, 1999). Experiments with purified feruloyl-pectins in vitro show that peroxidase + H_2O_2 or laccase can induce their gelation (Guillon and Thibault, 1990; Micard and Thibault, 1999; Oosterveld et al., 2000b, 2001). These experiments unambiguously demonstrate that inter-polymeric cross-links can be generated by these mechanisms although, as pointed out by Kerr and Fry (2004), they do not necessarily do so in living tissues. Another approach to seek evidence for inter-polysaccharide diFA cross-links is the correlation between the presence of the putative cross-link in vivo and the molecular size of the polysaccharide to which it is attached (Kerr and Fry, 2004). Using this approach, Oosterveld et al. (2002) provided some indications that sugar beet RG-I could be linked through the Ara side-chains, most probably by diFA cross-links.

Caryophyllales have been shown to be monophyletic using nucleotide sequences of the *rbc*L gene (quoted by Carnachan and Harris, 2000). Caryophyllale pectins studied so far (Rombouts and Thibault, 1986; Renard et al., 1993a, 1999) differ from the common blueprint of other dicotyledon pectins not only by high FA mono- and dimer contents, but also by high ''hairy'' regions/HG ratio and by high degree of acetylation. Arabinan and galactan side-chains are thought not to be randomly distributed over the RG-I backbone (Schols and Voragen, 1994) and the pectic composition of CW appears spatially regulated (Bush and McCann, 1999; Willats et al., 2001). Mazz et al. (2000) suggested that FA are not randomly distributed in sugar beet pectins and Obel et al. (2003) provided evidence that both feruloylated and non-feruloylated arabinoxylans were synthesized in cell suspension cultures of wheat (*Triticum aestivum* L. cv. Prelude). One can speculate that a huge spatial heterogeneity with respect to the degree of branching and FA and diFA esterification exists in sugar beet pectins. Indeed, the degree of polysaccharide cross-linking was shown to vary

widely among quinoa and sugar beet tissues with high diFA levels in roots compared to other tissues (Renard et al., 1999; Wende et al., 2000). Dimers could be present at high concentrations in epidermal cells and, in that case, might be involved in protecting the cells against damage by pathogens and/or soil abrasion (Wende et al., 2000). It was also suggested that dimers could be involved in controlling the overall growth of the plant (Wende et al., 2000; Yang and Uchiyama, 2000). Variations in diFA content of sugar beet tissues at different stages of development were also investigated (Wende et al., 1999, 2000). In the root, tissues laid down at the end of the growth period investigated (14 weeks) were much poorer in FA and diFA than those deposited early in root growth. It remains however unclear whether the proportion of the different diFA isomers varied during root maturation or not. In the present work, we have shown that in mature sugar beet roots, pectin cross-linking vary not only with respect to the diFA isomers involved, but also with respect to the nature of the sugar chains involved and the linkage position of the phenolic moieties to the sugar rings. This implies, as previously suggested (Wende et al., 2000), a remarkable degree of sophistication in the mechanisms which control polysaccharide cross-linking through diFA bridges. Furthermore, the dynamic nature of the plant CW includes a changing phenolic content and implies that the nature and extent of phenolic cross-linking are under close metabolic control (Wende et al., 1999). The recent isolation of a monoclonal antibody against feruloylated-β-D-(1 → 4)-galactan (Clausen et al., 2004) allows to envision the production of antibodies against some diFA-bridged oligosaccharides – whose structure was assessed in the present work – in order to study their distribution in planta.

It is highly unlikely that sugar beet pectins can be extensively cross-linked in situ by calcium ions in structures similar to egg-boxes (Renard et al., 1993b). Indeed, acetyl-esterification on top of methyl-esterification in the HG domains strongly hinders their associative properties through calcium ions (Ralet et al., 2003). Cross-linking through diFA bridges could constitute an alternative way of connecting those peculiar pectic molecules.

4. Experimental

4.1. Materials

The CWM was prepared from fresh mature sugar beet roots as previously described (Levigne et al., 2002). Driselase® was obtained from Sigma and Ronozym from Hoffman-La-Roche (Basel, Switzerland).

4.2. Isolation of diFA-rich fractions

CWM (10 g) was hydrolyzed by 0.05 M TFA (1 l) at 100 °C for 90 min. The hydrolysate was filtered on G4 sintered glass and the residue rinsed with distilled water. Supernatants were pooled and TFA was removed by three successive evaporation steps to dryness under vacuum at 40 °C. The supernatant was then solubilized in distilled water, precipitated by 4 volumes of ethanol and left overnight at 4 °C. The EtOH-soluble extract and precipitate were separated by centrifugation. After removal of EtOH by under vacuum evaporation at 40 °C, EtOH-soluble fraction was further hydrolyzed by 0.1 M TFA at 100 °C for 3 h. After removal of TFA, the hydrolysate was solubilised in distilled water and the pH brought to ~3 by 0.1 M NaOH. The EtOH-precipitate and the TFA hydrolysis residue were suspended in distilled water, brought to pH 5 by 0.1 M NaOH and hydrolyzed by a Driselase® (9.5 ml) and Ronozym® (0.1 ml) mixture for 24 h at 37 °C. Driselase® (678 mg) was suspended in distilled water (10 ml) and centrifuged. The supernatant solution was used. The hydrolysate was filtered on G3 sintered glass and the residue rinsed with distilled water. Supernatants were pooled and concentrated in vacuum.

Hydrolysates were loaded onto an Amberlite XAD-2 column (20 × 1.5 cm) eluted successively by water (3–4 column volumes), EtOH:water 15:85 (v/v) (3–4 column volumes), EtOH:water 25:75 (v/v) (3–4 column volumes) and EtOH:water 50:50 (v/v) (3–4 column volumes). Aliquots of selected fractions were concentrated to dryness, solubilized in distilled water (10 ml), brought to pH 2 by 1 M HCl and extracted twice by ether (25 ml). The aqueous phases were evaporated to dryness, solubilized in water (10 ml), brought to pH 4 by 0.1 M NaOH and loaded onto a column of Sephadex LH-20 (43 × 1.6 cm) eluted at ~35 ml/h successively by water (8 column volumes), EtOH:water 15:85 (4 column volumes) and EtOH:water 30:70 (8 column volumes). Fractions (9 ml) were collected and analyzed for their absorbance at 325 nm and colorimetrically for GalUA (Thibault, 1979) and total neutral sugars (Tollier and Robin, 1979). Selected fractions were pooled, concentrated and kept at −18 °C for further analysis.

4.3. General

The individual sugars were analyzed as their alditol acetate derivatives by gas chromatography after hydrolysis by 2 M TFA at 121 °C for 2 h (Blakeney et al., 1983). Hpaec was performed on a Dionex system with pulsed amperometric detection. The Carbopac PA1 column was eluted with 500 mM NaOH, 200 mM sodium acetate and water at 1 ml/min as follows: initial conditions, 20/30/50; 30 min, 20/60/20; 30–34 min, 20/60/20; 35 min, 20/30/50. Oligoarabinans were obtained by mild acid hydrolysis of sugar beet linearized arabinan (Megazyme) followed by size-exclusion chromatography (Bio-Gel P-2). Oligogalactans were obtained by mild acid hydrolysis of lupin type I arabinogalactan followed by size-exclusion chromatography (Bio-Gel P-2). Borwin software (JMBS Développements, Grenoble, France) was used for data acquisition and processing. Phenolic compounds were determined by hplc after saponification and ether extraction as previously

reported (Levigne et al., 2004b). Elution time and response factors relative to 3,4,5 trimethoxy-*trans*-cinnamic acid at 320 nm were established using commercial FA and diFA standards obtained as reported by Saulnier et al. (1999).

4.4. ^{18}O-Labeling

Reducing ends were ^{18}O-labeled by adding ~25 µl of $H_2{}^{18}O$ to ~25 µg of freeze-dried samples. Samples were incubated with $H_2{}^{18}O$ for ~90 h at ambient temperature in a dessicator.

4.5. Mass spectrometry

ESI-IT-MS experiments were achieved on an LCQ Advantage ion trap mass spectrometer (ThermoFinnigan, USA) using negative electrospray as the ionization process. Samples (^{18}O-labeled or not) were diluted in order to obtain a final concentration of 20–50 µg/ml in MetOH: water 1:1 (v/v). Infusion was performed at a flow rate of 2.5 µl/min. Nitrogen was used as sheath gas. No significant back-exchange of ^{16}O was observed during the analysis of the ^{18}O-labeled samples. The MS analyses were carried out under automatic gain control conditions, using a typical needle voltage of 4 kV and a heated capillary temperature of 200 °C. For MS^n experiments, the various parameters were adjusted for each sample in order to optimize signal and get maximal structural information from the ion of interest. More than 50 scans were summed for MS^n spectra acquisition. The Domon and Costello (1988) nomenclature was used to denote the fragment ions.

4.6. Molecular modeling

Molecular modeling was carried out on SGIs with the Accelrys©package. Molecular displays and energy minimizations used Insight II Biopolymer and Discover modules. The conformations were successively minimized using steepest descent (SD) and conjugate gradient (CG) minimization algorithms with the CVFF force field. The potential energy computed stretching, bending, torsion and electrostatic contributions as well as repulsion and dispersion of van der Waals interactions (Yiannikouris et al., 2004). The dielectric constant ε was 1 but all the final compounds were also minimized with ε 80 to compare data with implicite water.

4.6.1. Disaccharide construction

The global shape of α-L-Ara*f*-(1 → 5)-L-Ara*f* and β-D-Gal*p*-(1 → 4)-D-Gal*p* mainly depends on the rotation of the sugar rings around the glycosidic linkage (Perez et al., 2000). For α-L-Ara*f*-(1 → 5)-L-Ara*f*, the angles (φ_a, ψ_a, ω_a) described the glycosidic linkage with torsions between ($O–C_1–O_{5\prime}–C_{5\prime}$), ($C_1–O_{5\prime}–C_{5\prime}–C_{4\prime}$) and ($O_{5\prime}–C_{5\prime}–C_{4\prime}–O_\prime$), the prime indicating the reducing end. ω_a was known to adopt preferentially one of the staggered conformations (i) +60° (GG), (ii) −60° (GT) and (iii) +180° (TG) (Cros et al., 1993, 1994). For β-D-Gal*p*-(1 → 4)-D-Gal*p*, the (φ_g, ψ_g) angles of the glycosidic linkage were torsions between ($O–C_1–O_{4\prime}–C_{4\prime}$) and ($C_1–O_{4\prime}–C_{4\prime}–C_{5\prime}$). ($\varphi_a$, ψ_a, GG), (φ_a, ψ_a, GT), (φ_a, ψ_a, TG) and (φ_g, ψ_g) spaces were explored from −180° to +180° with a 10° step. The potential energy vs. torsion bonds was projected on final maps with contour to 10 kcal mol^{-1} above the minimum and a 2 kcal mol^{-1} step, then to 50 kcal mol^{-1} and a 10 kcal mol^{-1} step. For each disaccharide, the low energy conformations were identified and the second hydroxyl groups reconsidered through minimization. The final lowest energy conformation was kept further.

4.6.2. DiFA construction

The 8-O-4′ diFA contained torsion angles around which the FA monomers can rotate. The angles γ ($C_1–C_7–C_8–O_{4\prime}$) and λ ($C_7–C_8–O_{4\prime}–C_{4\prime}$) were explored from −180° to +180° with a 10° increment. Once this conformational minimum identified, the torsion bonds ($C_2–C_1–C_7–O_8$) and ($C_{3\prime}–C_{4\prime}–O_{4\prime}–C_{8\prime}$) were evaluated. That minimum was finally minimized (1000 iterations SD plus thousands of CG until normal completion). The 5-5′ diFA displayed no torsion bond and was directly minimized with the procedure described above.

4.6.3. Compound construction

To avoid multi dimensional hyperspace impossible to sample, the combination of fragments was stepwise. Any junction created between two fragments led to new rotational angles, explored from −180° to +180°, with a 10° increment. The lowest energy conformation was selected before the addition and torsion exploration of any ultimate fragment. Eventually, every complete compound was finally minimized through the procedure (see above). When the three fragments were bound together within every torsion angle positioned at its best, every complete compound was finally minimized through the abovementioned procedure.

Acknowledgments

The authors gratefully acknowledge the skillful technical assistance of Marie-Jeanne Crépeau. This study has been carried out with financial support from the Commission of the European Communities, specific RTD programme "Quality of Life and Management of Living Resources", proposal number QLK1-2002-02208 "Novel cross-linking enzymes and their consumer acceptance for structure engineering of foods", acronym CROSSENZ. It does not reflect its views and in no way anticipates the Commissions' future policy in this area.

Appendix A. Supplementary data

Supplementary data associated with this article can be found, in the online version, at doi:10.1016/j.phytochem.2005.09.039.

References

Blakeney, A.B., Harris, P.J., Henry, R.J., Stone, B.A., 1983. A simple and rapid preparation of alditol acetates for monosaccharide analysis. Carbohydr. Res. 113, 291–299.

Brady, J.D., Fry, S.C., 1997. Formation of di-isodityrosine and loss of isodityrosine in the cell walls of tomato cell-suspension cultures treated with fungal elicitors or H_2O_2. Plant Physiol. 115, 87–92.

Bush, M.S., McCann, M.C., 1999. Pectic epitopes are differentially distributed in the cell walls of potato (*Solanum tuberosum*) tubers. Physiol. Plant. 107, 201–213.

Carnachan, S.M., Harris, P.J., 2000. Ferulic acid is bound to the primary cell walls of all gymnosperm families. Biochem. Syst. Ecol. 28, 865–879.

Clausen, M.H., Ralet, M.-C., Willats, W.G.T., McCartney, L., Marcus, S.E., Thibault, J.-F., Knox, J.P., 2004. A monoclonal antibody to feruloylated-(1 → 4)-β-D-galactan. Planta 219, 1036–1041.

Colquhoun, I., Ralet, M.-C., Thibault, J.-F., Faulds, C.B., Williamson, G., 1994. Structure identification of feruloylated oligosaccharides from sugar-beet pulp by NMR spectroscopy. Carbohydr. Res. 263, 243–256.

Cros, S., Hervé du Penhoat, C., Perez, S., Imberty, A., 1993. Modeling of arabinofuranose and arabinan. Part I: conformational flexibility of the arabinose ring. Carbohydr. Res. 248, 81–93.

Cros, S., Imberty, A., Bouchemal, N., Hervé du Penhoat, C., Perez, S., 1994. Modeling of arabinofuranose and arabinan. Part II: nmr and conformational analysis of arabinose and arabinan conformational flexibility of the arabinose ring. Biopolymers 34, 1433–1447.

Domon, B., Costello, C.E., 1988. A systematic nomenclature for carbohydrate fragmentation in FAB-MS/MS spectra conjugates. Glycoconjugate J. 5, 397–409.

Fry, S.C., 1982. Phenolic components of the primary cell walls: feruloylated disaccharides of D-galactose and L-arabinose from spinach polysaccharide. Biochem. J. 203, 493–504.

Fry, S.C., 1986. Cross linking of matrix polymers in the growing cell walls of angiosperms. Annu. Rev. Plant Physiol. 37, 165–186.

Fry, S.C., Willis, S.C., Paterson, A.J., 2000. Intraprotoplasmic and wall-localised formation of arabinoxylan-bound diferulates and larger ferulate coupling-products in maize cell-suspension cultures. Planta 211, 679–692.

Guillon, F., Thibault, J.-F., 1989. Methylation analysis and mild acid hydrolysis of the "hairy" fragments of sugar beet pectins. Carbohydr. Res. 190, 85–96.

Guillon, F., Thibault, J.-F., Rombouts, F.M., Voragen, A.G.J., Pilnik, W., 1989. Enzymic hydrolysis of the "hairy" fragments of sugar-beet pectins. Carbohydr. Res. 190, 97–108.

Guillon, F., Thibault, J.-F., 1990. Oxidative cross-linking of chemically and enzymatically modified sugar-beet pectin. Carbohydr. Polym. 12, 353–374.

Harvey, D.J., 2000. Collision-induced fragmentation of underivatised carbohydrates ionized by electrospray. J. Mass Spectrom. 35, 1178–1190.

Hatfield, R.D., Ralph, J., 1999. Modelling the feasability of intramolecular dehydrodiferulate formation in grass walls. J. Sci. Food Agric. 79, 425–427.

Ishii, T., 1991. Isolation and characterization of a diferuloyl arabinoxylan hexasaccharide from bamboo shoot cell-walls. Carbohydr. Res. 219, 15–22.

Ishii, T., Tobita, T., 1993. Structural characterization of feruloyl oligosaccharides from spinach-leafs cell walls. Carbohydr. Res. 248, 179–190.

Janaswami, S., Chandrasekaran, R., 2005. Polysaccharide structures from powder diffraction data: molecular models of arabinan. Carbohydr. Res. 340, 835–839.

Kamisaka, S., Takeda, S., Takahashi, K., Shibata, K., 1990. Diferulic and ferulic acid in the cell wall of *Avena* coleoptiles – their relationships to mechanical properties of the cell wall. Physiol. Plant. 78, 1–7.

Kerr, E.M., Fry, S.C., 2004. Extracellular cross-linking of xylan and xyloglucan in maize cell-suspension cultures: the role of oxidative phenolic coupling. Planta 219, 73–83.

Levigne, S., Ralet, M.-C., Thibault, J.-F., 2002. Characterisation of pectins extracted from fresh sugar beet under different conditions using an experimental design. Carbohydr. Polym. 49, 145–153.

Levigne, S.V., Ralet, M.-C.J., Quéméner, B.C., Pollet, B.M.-L., Lapierre, C., Thibault, J.-F.J., 2004a. Isolation from sugar beet cell walls of arabinan oligosaccharides esterified by two ferulic acid monomers. Plant Physiol. 134, 1173–1180.

Levigne, S., Ralet, M.-C., Quéméner, B., Thibault, J.-F., 2004b. Isolation of diferulic bridges ester-linked to arabinan in sugar beet cell walls. Carbohydr. Res. 339, 2315–2319.

Mazz, M., McCann, M.C., Kolpak, F., White, A.R., Stacey, N.J., Roberts, K., 2000. Extraction of pectic polysaccharides from sugar-beet cell walls. J. Sci. Food Agric. 80, 17–28.

Micard, V., Grabber, J.H., Ralph, J., Renard, C.M.G.C., Thibault, J.-F., 1997. Dehydrodiferulic acids from sugar-beet pulp. Phytochemistry 44, 1365–1368.

Micard, V., Thibault, J.-F., 1999. Oxidative gelation of sugar-beet pectins: use of laccases and hydration properties of the cross-linked pectins. Carbohydr. Polym. 39, 265–273.

Mort, A.J., 2002. Interactions between pectins and other polymers. In: Seymour, G.B., Knox, J.P. (Eds.), Pectins and their Manipulation. Blackwell Publishing CRC Press, Oxford, pp. 30–51.

Obel, N., Porchia, A.C., Scheller, H.V., 2003. Intracellular feruloylation of arabinoxylan in wheat: evidence for feruloyl-glucose as precursor. Planta 216, 620–629.

Oosterveld, A., Beldman, G., Schols, H.A., Voragen, A.G.J., 2000a. Characterization of arabinose and ferulic acid rich pectic polysaccharides and hemicelluloses from sugar beet pulp. Carbohydr. Res. 328, 185–197.

Oosterveld, A., Beldman, G., Voragen, A.G.J., 2000b. Oxidative cross-linking of pectic polysaccharides from sugar beet pulp. Carbohydr. Res. 328, 199–207.

Oosterveld, A., Pol, I.E., Beldman, G., Voragen, A.G.J., 2001. Isolation of feruloylated arabinans and rhamnogalacturonans from sugar beet pulp and their gel forming ability by oxidative cross-linking. Carbohydr. Polym. 44, 9–17.

Oosterveld, A., Beldman, G., Voragen, A.G.J., 2002. Enzymatic modification of pectic polysaccharides obtained from sugar beet pulp. Carbohydr. Polym. 48, 73–81.

Perez, S., Mazeau, K., Hervé du Penhat, C., 2000. The three-dimensional structures of the pectic polysaccharides. Plant Physiol. Biochem. 38, 37–55.

Quéméner, B., Ralet, M.-C., 2004. Evidence for linkage position determination in known feruloylated mono- and disaccharides using electrospray ion trap mass spectrometry. J. Mass Spectrom. 39, 1153–1160.

Ralet, M.-C., Thibault, J.-F., Faulds, C.B., Williamson, G., 1994. Isolation and purification of feruloylated oligosaccharides from cell walls of sugar-beet pulp. Carbohydr. Res. 263, 227–241.

Ralet, M.-C., Crépeau, M.-J., Buchholt, H.-C., Thibault, J.-F., 2003. Polyelectrolyte behaviour and calcium binding properties of sugar beet pectins differing in their degrees of methylation and acetylation. Biochem. Eng. J. 16, 191–201.

Ralph, J., Helm, R.F., 1993. Lignin/hydroxycinnamic acid/polysaccharide complexes: synthetic models for regio/chemical characterization. In: Jung, H.G., Buxton, D.R., Hatfield, R.D., Ralph, J. (Eds.), Forage Cell Wall Structure and Digestibility. ASA-CSSA-SSSA, Madison, pp. 201–246.

Renard, C.M.G.C., Champenois, Y., Thibault, J.-F., 1993a. Characterization of the extractable pectins and hemicelluloses of the cell wall of glasswort, *Salicornia ramosissima*. Carbohydr. Polym. 22, 239–245.

Renard, C.M.G.C., Thibault, J.-F., Liners, F., Van Cutsem, P., 1993b. Immunological probing of pectins isolated or in situ. Acta Bot. Neerl. 42, 199–204.

Renard, C.M.G.C., Wende, G., Booth, E.J., 1999. Cell wall phenolics and polysaccharides in different tissues of quinoa (*Chenopodium quinoa* Willd). J. Sci. Food Agric. 79, 2029–2034.

Rombouts, F.M., Thibault, J.-F., 1986. Feruloylated pectic substances from sugar-beet pulp. Carbohydr. Res. 154, 177–187.

Saulnier, L., Crépeau, M.-J., Lahaye, M., Thibault, J.-F., Garcia-Conesa, M.T., Kroon, P.A., Williamson, G., 1999. Isolation and structural determination of two 5-5′ diferuloyl oligosaccharides indicate that maize heteroxylans are covalently cross-linked by oxidatively coupled ferulates. Carbohydr. Res. 320, 82–92.

Schols, H.A., Voragen, A.G.J., 1994. Occurrence of pectic hairy regions in various plant cell wall materials and their degradability by rhamnogalacturonase. Carbohydr. Res. 256, 83–95.

Thibault, J.-F., 1979. Automated-method for the determination of pectic substances. Lebensm.-Wiss. u.-Technol. 12, 247–251.

Tollier, M.-T., Robin, J.-P., 1979. Adaptation of the orcinol-sulfuric acid method for the automatic titration of total neutral sugars – conditions of application to plant extracts. Ann. Technol. Agric. 28, 1–15.

Vakhrushev, S.Y., Zamfir, A., Peter-Katalinic, J., 2004. $^{0,2}A_n$ cross-ring cleavage as a general diagnostic tool for glycan assignment in glycoconjugate mixtures. J. Am. Soc. Mass Spectrom. 15, 1863–1868.

Vyas, N.K., 1991. Atomic features of protein–carbohydrate interactions. Curr. Opin. Struct. Biol. 1, 732–740.

Waldron, K.W., Ng, A., Parker, M.L., Parr, A.J., 1997. Ferulic acid dehydrodimers in the cell walls of *Beta vulgaris* and their possible role in texture. J. Sci. Food Agric. 74, 221–228.

Wende, G., Waldron, K.W., Smith, A.C., Brett, C.T., 1999. Developmental changes in cell-wall ferulate and dehydrodiferulates in sugar beet. Phytochemistry 52, 819–827.

Wende, G., Waldron, K.W., Smith, A.C., Brett, C.T., 2000. Tissue-specific developmental changes in cell-wall ferulate and dehydrodiferulates in sugar beet. Phytochemistry 55, 103–110.

Willats, W.G.T., McCartney, L., Mackie, W., Knox, J.P., 2001. Pectin: cell biology and prospects for functional analysis. Plant Mol. Biol. 47, 9–27.

Yang, J.-G., Uchiyama, T., 2000. Hydroxycinnamic acids and their dimers involved in the cessation of cell elongation in *Mentha* suspension culture. Biosci. Biotech. Bioch. 64, 1572–1579.

Yiannikouris, A., André, G., Buléon, A., Jeminet, G., Canet, I., François, J.M., Bertin, G., Jouany, J.P., 2004. Comprehensive conformational study of key interactions involved in zearalenone complexation with β-D-glucans. Biomacromolecules 5, 2176–2185.